

University of Montana

ScholarWorks at University of Montana

Water Topos: A 3-D Trend Surface Approach to
Viewing and Teaching Aqueous Equilibrium
Chemistry

Open Educational Resources (OER)

1-2022

Chapter 3.2: Why Batteries Deliver a Fairly Constant Voltage Until They Suddenly Die: An Application of Nernst Topo Surfaces

Garon C. Smith

University of Montana, Missoula

Md Mainul Hossain

North South University, Bangladesh

Patrick MacCarthy

Colorado School of Mines

Follow this and additional works at: <https://scholarworks.umt.edu/topos>

 Part of the [Chemistry Commons](#)

Let us know how access to this document benefits you.

Recommended Citation

Smith, Garon C.; Hossain, Md Mainul; and MacCarthy, Patrick, "Chapter 3.2: Why Batteries Deliver a Fairly Constant Voltage Until They Suddenly Die: An Application of Nernst Topo Surfaces" (2022). *Water Topos: A 3-D Trend Surface Approach to Viewing and Teaching Aqueous Equilibrium Chemistry*. 9.
<https://scholarworks.umt.edu/topos/9>

This Book is brought to you for free and open access by the Open Educational Resources (OER) at ScholarWorks at University of Montana. It has been accepted for inclusion in Water Topos: A 3-D Trend Surface Approach to Viewing and Teaching Aqueous Equilibrium Chemistry by an authorized administrator of ScholarWorks at University of Montana. For more information, please contact scholarworks@mso.umt.edu.

Chapter 3.2

Why Batteries Deliver a Fairly Constant Voltage Until They Suddenly Die: An Application of Nernst Topo Surfaces

Garon C. Smith¹, Md Mainul Hossain² and Patrick MacCarthy³

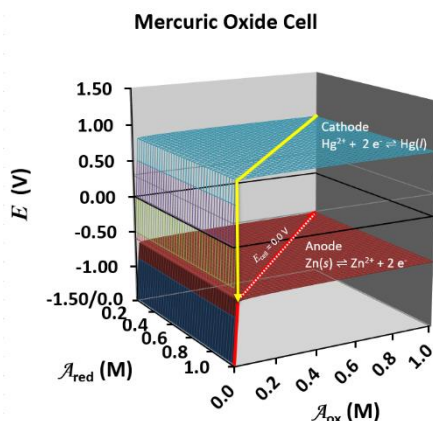
¹Department of Chemistry and Biochemistry, University of Montana, Missoula, MT 59812, USA

²Department of Biochemistry and Microbiology, North South University, Dhaka 1229, Bangladesh

³Department of Chemistry and Geochemistry, Colorado School of Mines, Golden, CO 80401, USA

Abstract

Two characteristics of batteries, their delivery of nearly constant voltage and their rapid failure, are explained through a visual examination of the Nernst equation. Two Galvanic cells are described in detail: (1) a wet cell involving iron and copper salts and (2) a mercury oxide dry cell. A complete description of the wet cell requires a three-dimensional Nernst surface because the potential is a function of two variables: the activities of both the oxidized and reduced forms in each redox couple. Dry cell potentials, which utilize solid or pure liquid species, are functions of only one variable and can be described by a pair of traces in a traditional plot. Plots of the Nernst potential are relatively flat for most activities, but they exhibit bluffs and cliffs under extreme conditions. The flat plateaus are responsible for the fairly constant voltage that batteries deliver; the bluffs and cliffs explain why batteries fail so quickly as they wear down. This chapter, an expansion of ideas introduced in Chapter 3.1, focuses on a familiar real-world application.



3.2.1 Introduction

(NOTE: This chapter is an updated version of the first topo surface paper that we published.¹ Chapter 3.1 develops the redox composition grid concept in full. Because of that, parts of this chapter are a brief repeat of some of its content. We retain them in a spirit of maintaining the structure of the original paper.)

Have you ever wondered why batteries seem to be working fine right up to the moment that they fail? You get a warning “low battery” and shortly thereafter, your electronic device quits working. Hopefully, you backed up your data and you have some spare batteries to install. Once you are close to failure, batteries slip from “weak” to “dead” in a very short time. So how can the batteries be okay one minute and not the next? To understand how batteries behave, one must understand how the Nernst equation dictates the voltages produced in a galvanic cell. After all, batteries are a nothing more than a type of galvanic cell. This chapter shows how the voltage behaves over the lifespan of a battery. The voltage is fairly constant until it suddenly plummets as one (or both) of the component species is exhausted.

3.2.2 The Nernst Equation Viewed as a Surface

The Nernst equation^{2,3} for a half-reaction is typically given as

$$E = E^0 + \frac{RT}{nF} \ln \frac{\mathcal{A}_{\text{ox}}^a}{\mathcal{A}_{\text{red}}^b} \quad (3.2-1)$$

where E is the half-cell potential expressed in volts, E^0 is the half-cell's standard reduction potential for unit activity and 298 K, R is the universal gas constant, T is the absolute temperature in kelvin, n is the number of electrons transferred in the half-reaction, F is the Faraday constant, \mathcal{A}_{ox} is the activity of the oxidized form of the redox couple, \mathcal{A}_{red} is the activity of the reduced form of the redox couple, and a and b are stoichiometric factors from the half-reaction's coefficients for the oxidized and reduced forms, respectively. The two most important terms in eq 3.2-1 on which to focus are: 1) the standard reduction potential of the half-

reaction, E^0 ; and 2) the logarithmic term, $\ln(\mathcal{A}_{\text{ox}}/\mathcal{A}_{\text{red}})$. The E^0 largely controls the voltage of a half-reaction while the battery is “doing fine”. As the battery is “failing”, the logarithmic term suddenly dominates. The interplay between the two terms becomes easy to see when you view a three-dimensional plot of the Nernst equation using linear axes that extend to relatively high activities. Its appearance also depends on whether the species involved in the half-reaction are in aqueous solution versus in a solid or pure liquid state.

We will begin with a wet cell that corresponds to half-reactions for which both the oxidized and reduced forms of the redox couple are present in the aqueous phase. To look at all possible voltages that an aqueous redox couple could generate, we need to build a grid that holds the full range of activities for both forms. The range of the oxidized form’s activity will be indicated on the y -axis and the range of the reduced form’s activity on the x -axis. The two axes represent the balance between the oxidized and reduced forms of the substance comprising a redox couple. Substituting a specific ratio of $\mathcal{A}_{\text{ox}}/\mathcal{A}_{\text{red}}$ into the Nernst equation generates a single voltage, E . A systematic substitution of many $\mathcal{A}_{\text{ox}}/\mathcal{A}_{\text{red}}$ ratios that cover the full activity range of both forms yields a collection of voltages that can be plotted on a z -axis above the grid. This set of voltages collectively describes a three-dimensional picture of the Nernst equation behavior. Figure 3.2-1 illustrates the Nernst potential “topo” surface for the half reaction:

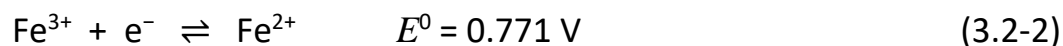
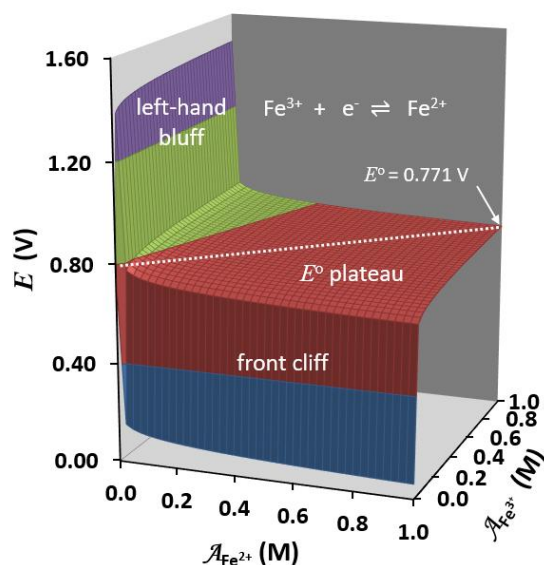


Figure 3.2-1. The Nernst topo surface for the $\text{Fe}^{3+}/\text{Fe}^{2+}$ half-reaction with the E^0 and its associated plateau noted. All E^0 values for this paper are taken from reference 4.



What is compellingly obvious in looking at the Nernst potential surface in Figure 3.2-1 is that a large portion of it is flat. What is more, the voltage corresponding to the flat region is centered fairly close to 0.771 V, the E^0 value! Thus, we call it the E^0 plateau (as in Chapter 3.1). The definition of E^0 is shown as the grid point at the right-hand back corner of the surface – the point at which both $\mathcal{A}_{\text{Fe}^{2+}}$ and $\mathcal{A}_{\text{Fe}^{3+}}$ are at unit activity, 1.0 M. Given the linear axes of the grid, the voltage for a redox couple never moves far from the E^0 value over most ratios of Fe^{3+} to Fe^{2+} . It is only when either $\mathcal{A}_{\text{Fe}^{2+}}$ or $\mathcal{A}_{\text{Fe}^{3+}}$ approach extremely small values that the potential begins to change. Once there, however, the change is dramatic; it rises or falls at an exponential rate. In fact, the surfaces along both axes have been artificially truncated by using an activity of 1.0×10^{-24} M instead of 0.0 M. At activities of 0, the surface would rise to $+\infty$ along the y -axis and drop to $-\infty$ along the x -axis. The Nernst equation basically says that E^0 is the predominant contributor to the potential for a linear grid's surface everywhere except immediately adjacent to the two axes. As will become apparent later in this chapter, the flatness of a linear grid's Nernst potential surface for most $\mathcal{A}_{\text{ox}}/\mathcal{A}_{\text{red}}$ ratios is responsible for the relatively steady voltage delivered by a battery during its working life.

The second term on the right-hand side of eq 3.2-1, namely

$$\frac{RT}{nF} \ln \frac{\mathcal{A}_{\text{ox}}^a}{\mathcal{A}_{\text{red}}^b} \quad (3.2-3)$$

is an “adjustment factor” for fluctuations in the ratio of the oxidized and reduced forms. It does not have much impact on the computed value of E when the $\mathcal{A}_{\text{ox}}/\mathcal{A}_{\text{red}}$ ratio is fairly close to unity. With linear axes, the impact is small for most grid points. Because the activity ratio is preceded by a natural logarithm operator and the natural logarithm of 1 is equal to 0, not much voltage adjustment is needed until the ratio departs significantly from 1. Furthermore, the coefficient preceding the logarithmic term is equal to 0.05917 at 298 K. Unless the $\mathcal{A}_{\text{ox}}/\mathcal{A}_{\text{red}}$ ratio has changed greatly, its impact is further attenuated by this small coefficient.

A detailed examination of the plateau region for this specific case reveals that equipotential lines radiate outward from the origin like spokes on a wheel because these denote constant values for the $\mathcal{A}_{\text{ox}}/\mathcal{A}_{\text{red}}$ ratio. In fact, the line

between the origin and E^0 is the locus of points for which $\mathcal{A}_{\text{Fe}^{2+}} = \mathcal{A}_{\text{Fe}^{3+}}$ and the second term of the Nernst equation goes to zero. Points to the right of that line are slightly lower than E^0 and points to the left are slightly higher.

As soon as one form of the redox couple is nearly depleted, the “adjustment factor” suddenly becomes an important determiner of the half-cell potential. The act of discharging a galvanic cell corresponds to moving diagonally toward one axis or the other at a steady rate. Thus, when the “left-hand bluff” or the “front cliff” is approached, any additional movement quickly changes the half-cell potential. This rapid change in potential is responsible for the quick demise of a failing battery.

3.2.3 Galvanic Cells

A galvanic cell involves two half-reactions, one for the anode half-cell and one for the cathode half-cell, so two Nernst surfaces are needed to display the sequence of potentials that occur as a cell operates. For purposes of illustration, consider a wet-chemistry-based galvanic cell in which Fe^{3+} at unit activity in one half-cell oxidizes Cu^+ at unit activity in the other half-cell (Figure 3.2-2).

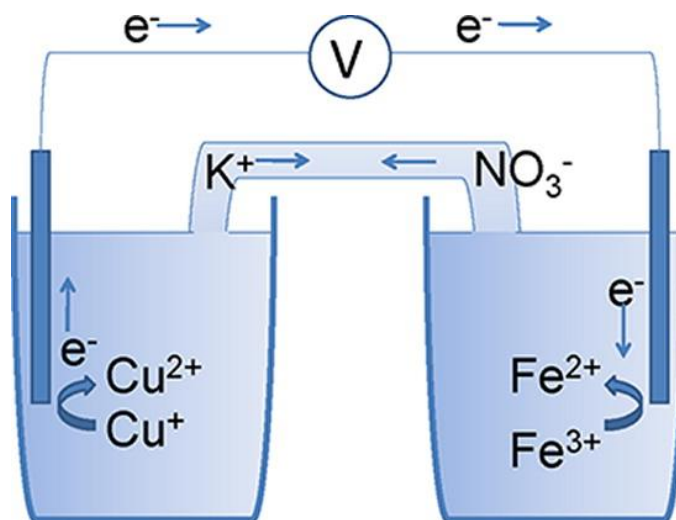
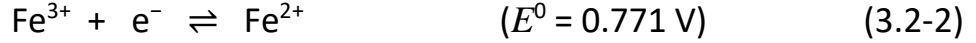
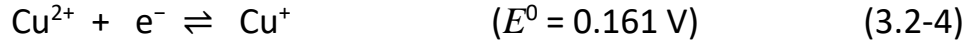


Figure 3.2-2. A schematic diagram for the $\text{Fe}^{3+}/\text{Cu}^+$ galvanic cell. The Fe^{3+} half-cell is the cathode; the Cu^+ half-cell is the anode. A KNO_3 salt bridge connects the two half-cells.

The cathode reaction, where reduction occurs, is given by the same iron redox couple cited earlier, namely,



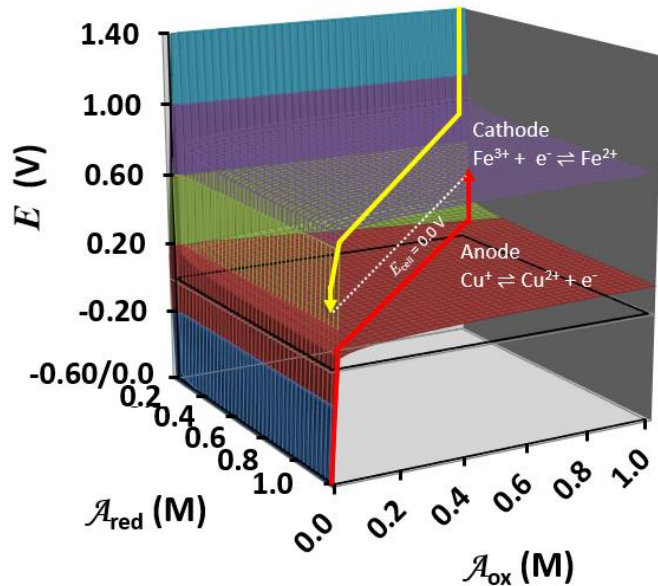
and the anode, where oxidation takes places and which runs in the reverse direction, is given by the standard reduction half-reaction



Note that the spontaneous reaction required for a galvanic cell has the half-reaction with the lower E^0 as the anode.

Just as it takes two half-cells to form a Galvanic cell, it takes two Nernst surfaces to illustrate the behavior of the pair of half-cell potentials that accompany its operation (Figure 3.2-3). The upper Nernst surface represents the iron half-cell; the lower surface represents the copper half-cell.

Figure 3.2-3. The paired Nernst surfaces depicting the $\text{Fe}^{3+}/\text{Cu}^{+}$ galvanic cell. Upper surface: $\text{Fe}^{3+}/\text{Fe}^{2+}$; lower surface $\text{Cu}^{2+}/\text{Cu}^{+}$. $E_{\text{cell}} = 0$ when both surface potentials are 0.466 V.



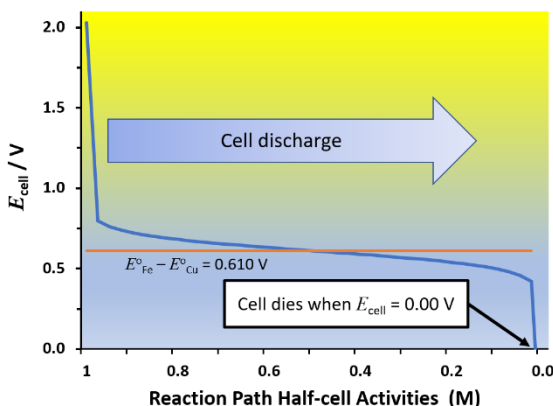
The reduction path (shown in yellow on the upper surface) starts with the Fe^{3+} at unit activity and Fe^{2+} essentially absent. As the Fe^{3+} is consumed, it is converted to Fe^{2+} . Thus, the ratio of $\mathcal{A}_{\text{Fe}^{3+}}/\mathcal{A}_{\text{Fe}^{2+}}$ moves diagonally down and to the right on the composition grid. The potential drops almost instantaneously from an initial high value on the left-hand bluff down to a value near E^0 on the flat plateau area of the Fe top. It continues at this general level until the Fe^{3+} is nearly depleted.

The lower Nernst surface represents the copper half-cell. The oxidation path (shown in red) starts with Cu^+ at unit activity and Cu^{2+} essentially absent. As the cell operates, the Cu potential rapidly ascends to the E^0 plateau region of the Cu topo. It continues at this general level until Cu^+ is nearly depleted.

The galvanic discharge reaction continues to be spontaneous as long as the iron half-cell potential is greater than that in the copper half-cell potential. Because the entire $\text{Fe}^{3+}/\text{Fe}^{2+}$ plateau is well above that for $\text{Cu}^{2+}/\text{Cu}^+$, the reaction path moves diagonally across the surface until it hits the front cliff. When the Fe^{3+} is nearly depleted, the potential quickly plummets. The Cu^+ oxidation path rises from its start on the front cliff, progresses diagonally across its plateau to its left-hand bluff, and then begins to rapidly climb when the Cu^+ is nearly gone. The galvanic cell reaction stops (*i.e.*, “dies”) when the dropping Fe^{3+} path and the rising Cu^+ path achieve the same potential. Given the symmetry of these two hypothetical half-cell reactions, this happens simultaneously and the equilibrium point corresponds to a potential exactly half-way between the two plateaus, that is, $E_{\text{Fe}} = E_{\text{Cu}} = (0.771 + 0.161)/2 = 0.466 \text{ V}$.

Figure 3.2-3 supports the situation promised in the title of this chapter. The voltage delivered by an operating cell is dictated by E_{cell} , the vertical spacing between the two, colored discharge reaction paths. Because the paths primarily traverse essentially horizontal planes, the voltage difference is nearly constant. This can be seen in Figure 3.2-4. The E_{cell} is centered around $E^0_{\text{Fe}} - E^0_{\text{Cu}} = 0.771 \text{ V} - 0.161 \text{ V} = 0.610 \text{ V}$.

Figure 3.2-4. The E_{cell} values for the $\text{Fe}^{3+}/\text{Cu}^+$ galvanic cell during discharge



The reason a battery suddenly dies is a result of the discharge paths leaving the planar portion of the Nernst surfaces. When a reduction path drops over the

front cliff or an oxidation path rapidly climbs up the left-hand bluff or both, the voltage difference rapidly diminishes to zero and the cell dies. Given a constant current draw on the cell, the rapid voltage change happens over a very short stretch of the reaction path. It is a “sudden death” phenomenon.

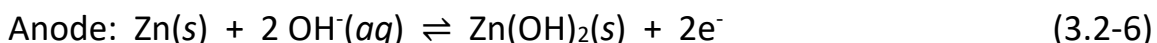
3.2.4 Batteries Utilizing Solid or Pure Phase Redox Species

Nernst potentials for dry cell batteries are vastly simpler in appearance than those for wet cells. This is because the variables in the logarithmic term of the Nernst equation are restricted to aqueous species. The activity of a solid phase or a pure liquid phase is defined as unity. The Nernst potential for these reactions is often a function of only one redox species. Thus, a single trace captures the series of potentials that are encountered during a discharge event. A surface is not necessarily needed.

As an illustrative example, consider the mercuric oxide battery that was commonly used for watches, cameras, and pacemakers until environmental disposal concerns led to its being phased out.⁵ The half-reactions for a mercuric oxide cell are typically given as⁶

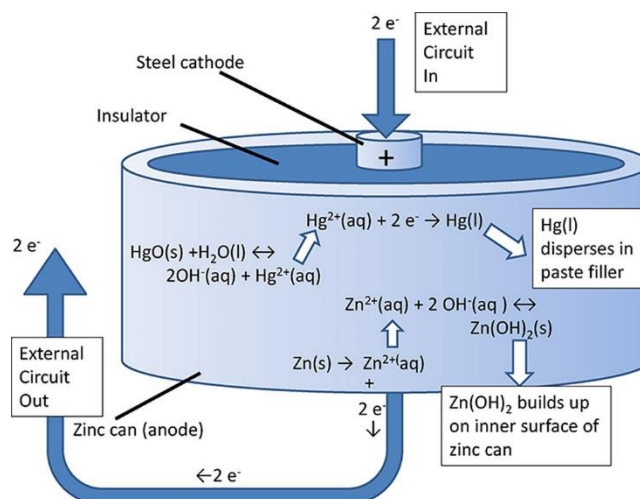


and

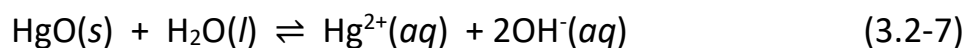


Both reactions are really net reactions for two-step processes that are depicted in a schematic diagram (Figure 3.2-5) and expanded below. Even though these batteries are referred to as dry cells, they usually have some liquids present in a paste or gelled state. This is apparent from the presence of the $\text{OH}^-(aq)$ species in both eqs 3.2-5 and 3.2-6.

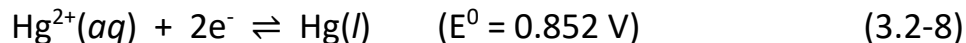
Figure 3.2-5. Schematic diagram of the mercuric oxide dry cell. Chemical reactions illustrate the two-step process at each electrode.



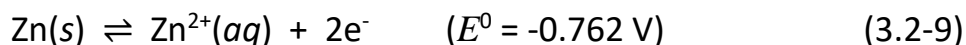
The cathode reaction involves a dissolution step:



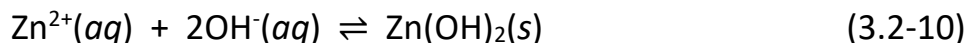
and then a reduction step:



The anode reaction involves a redox step:



followed immediately by a precipitation event:



As the battery discharges, mercuric oxide dissolves to a slight extent and the Hg^{2+} ions formed can then pick up electrons from the cathode and change into liquid mercury. The liquid mercury disperses throughout the paste or gel-filled core of the battery. (If the mercury did not disperse, the cell could be rechargeable.) The zinc “can” of the battery is converted into zinc hydroxide (or zinc oxide) that coats the inside of the remaining zinc can.

The Nernst potentials are predominantly regulated by the two redox half-reactions shown as eqs 3.2-8 and 3.2-9. A plot with two traces is sufficient to display the series of potentials that occur during a mercuric oxide battery discharge (Figure 3.2-6). The upper trace represents the reduction half-cell potentials of the cathode whereas the lower trace follows the oxidation half-cell potentials of the anode. The theoretical voltage available between eqs 3.2-8 and 3.2-9 is $(0.852 \text{ V}) - (-0.762 \text{ V}) = 1.614 \text{ V}$. Generally, mercury cells deliver an open circuit voltage of about 1.4 V due to resistance losses, differences in ion mobilities, accumulation of species at the metal electrode surfaces, and circuit overpotentials. A plot of E_{cell} voltages during discharge (Figure 3.2-7) again provides a visual explanation for the cell behavior. First, as there is essentially a constant vertical difference between the two traces over most of the discharge path, the cell output voltage will be relatively constant. Second, the battery will die suddenly because the upper mercury trace exponentially drops when Hg^{2+} is depleted. When the plunging upper mercury trace hits the essentially constant potential of zinc's lower E^0 plateau, the cell dies.

Figure 3.2-6. The half-cell potentials as the Hg^{2+}/Zn galvanic cell discharges.

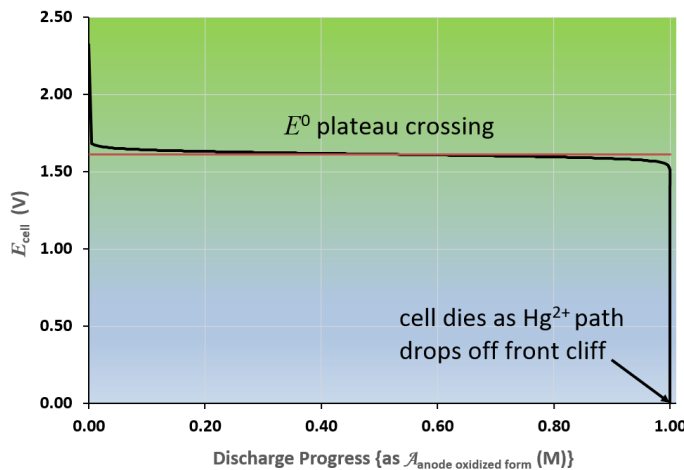
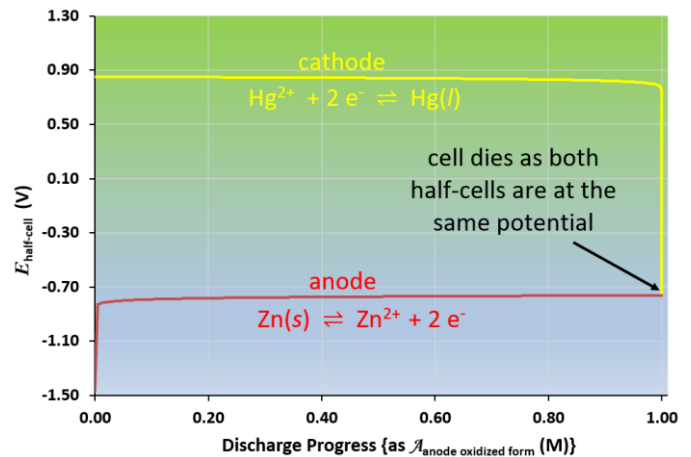


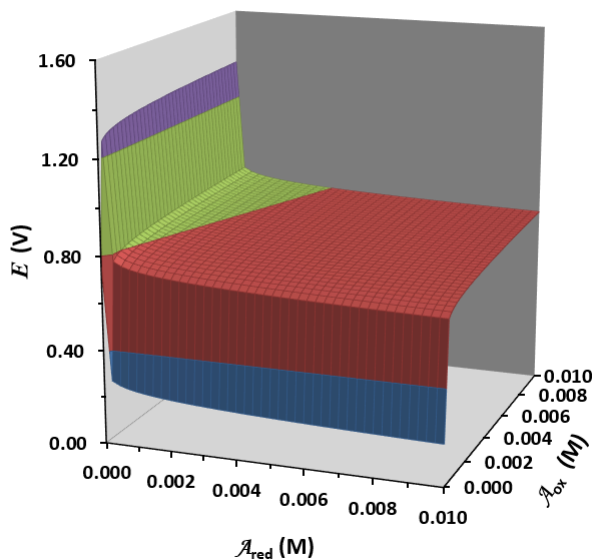
Figure 3.2-7. The E_{cell} values during discharge

3.2.5 Some Additional Teaching Points with Nernst Surfaces

Galvanic cells are a frequently encountered topic in chemical education.⁷⁻¹¹ Their use typically falls into one of two categories: use for a source of energy as batteries¹² or use in analytical measurements via pH or ion selective electrodes.¹³⁻¹⁶ The Nernst surface approach provides a nice way to contrast how the potentials are used in the two applications by illustrating the difference between displaying the Nernst equation on linear versus logarithmic scales. Battery applications are best understood using a linear composition grid; analytical measurements employing electrodes are best understood using a logarithmic composition grid.

The surface shown in Figure 3.2-1 has linear grid axes that extend to 1.0 M, a large value compared to those found in most real solutions. This was done expressly to illustrate the grid point that defines the E^0 conditions. The Nernst surface looks the same for smaller ranges of activities as long as it is still plotted on a linear set of axes. Restriction of the activity range to a maximum value of 0.01 M makes essentially no perceptible difference in the appearance of the Nernst surface (Figure 3.2-8).

Figure 3.2-8. The $\text{Fe}^{3+}/\text{Fe}^{2+}$ Nernst surface with a maximum activity of 0.01 M.



The region of rapid change is still completely contained within the first and last grid intervals. The potentials generated by the Nernst equation will be dominated by E^0 whenever they are plotted on linear grid axes and are associated with the relatively high levels of ions that are present in batteries. The logarithmic

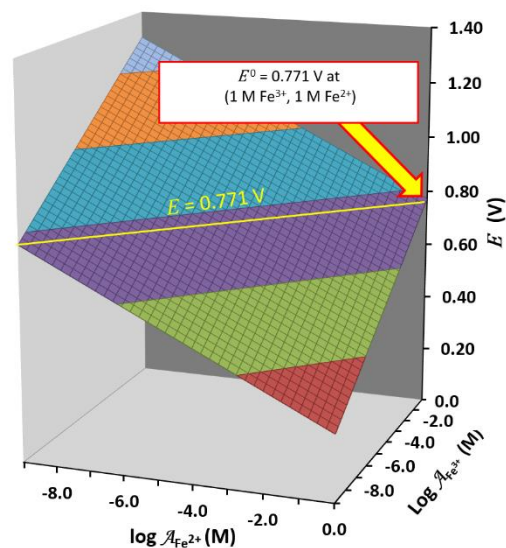
term is only a minor contributor until battery failure. An analogous effect is seen in acid–base chemistry with the Henderson–Hasselbalch equation¹⁷ and the pH value associated with a buffer solution:

$$\text{pH} = \text{p}K_a + \log \frac{[\text{base form}]}{[\text{acid form}]} \quad (3.2-11)$$

When significant quantities of both an acid and its conjugate base form are present, it is largely the $\text{p}K_a$ value that determines a buffer's pH, not the logarithmic term that contains the ratio of acid- to base-forms. A buffer possesses a relatively stable value until its capacity is exceeded. Then, it, too, shows rapid pH changes.

Plotting the Nernst surface over a logarithmic grid reveals an entirely different look. The logarithmic axes yield a sloped Nernst surface that is perfectly planar (Figure 3.2-9). The planar behavior is the basis for another extremely powerful application of the Nernst equation, namely, employing the observed potential of a sensing electrode to measure the activity of an aqueous analyte. The logarithmic scales permit useful information to be extracted over many orders of magnitude. We selected 1×10^{-9} M to 1 M in this figure to include the working range of most commercial ion selective electrodes. Electrodes for determining pH, for example, depend on a linear response of 59.17 mV for each order of magnitude change in H_3O^+ activity. The sensing electrode is one half-cell in a galvanic cell. The other half of the galvanic cell is maintained at a constant potential by means of a reference half-cell, typically Ag/AgCl. All change in the overall cell potential is attributable to the change in the analyte activity. Other ion selective electrodes have been developed to follow the activities of a number of charged species in solution such as Cl^- , F^- , Cu^{2+} , and Ag^+ .

Figure 3.2-8. The Nernst surface for the $\text{Fe}^{3+}/\text{Fe}^{2+}$ half-reaction plotted above a grid with logarithmic axes.



For upper-level analytical courses, the linear surfaces give a unique visualization of exactly what E^0 represents. The conditions that define E^0 are not a very practical solution and it is unlikely that they will be encountered in an actual experiment. On the other hand, it is quite likely that a potential equal to E^0 will be encountered when identical activities of the oxidized and reduced forms are present, such as half way to an equivalence point in a redox titration. Students should realize that the diagonal locus of points from the origin to E^0 (at the 1.0 M, 1.0 M grid point) are all equipotential for this 1:1 stoichiometric relationship between the oxidized and reduced forms. For other stoichiometries, the equipotential traces will be curved lines emanating from the origin.

Finally, the concept of mapping experimental paths onto a composition grid forces students to consider the sequence of compositional changes that relate to procedures carried out on a system.¹⁸ The redox paths shown in this chapter, that correspond to cell discharges, form traces that angle across the grid with negative slopes. They are easy to understand because there are no volume changes that accompany the redox reactions. If you ask the students to characterize what happens during a dilution procedure on the linear grid for a 1:1 stoichiometry, they should respond with a path that tracks from its starting coordinates and proceeds straight toward the origin. Because the ratio of oxidized to reduced form does not change, all points will be at an equipotential voltage. A more challenging exercise would ask students to plot the experimental path for a redox titration.

The use of composition grids helps students visualize the behavior of an aqueous equilibrium concept over a universe of possible concentrations. Realizing how compositions of a system change during experimental procedures such as titrations or dilutions will deepen their appreciation of some subtle points. These were explored in earlier chapters.

3.2.6 Conclusions

Two important characteristics of batteries, near constant voltage and quick deaths, are a consequence of the Nernst equation. The Nernst equation, when plotted as a 3-D surface above a linear composition grid, shows essentially two types of features. Much of it is a flattish plateau and the edges are cliffy. Flat

spots are responsible for the near constancy of the voltage. The voltage for a half-cell remains quite close to its E^0 value over most of its useful life because drawing a current (a linear process) only makes small changes in species' activities. Furthermore, the impacts of these small changes are damped by the logarithmic nature of the second term in the Nernst equation (eq 3.1-1) and its small coefficient of 0.05917. It is only when a redox species is nearly depleted, that drawing a current can suddenly change its activity by orders of magnitude. Under these conditions, the logarithmic term quickly goes from being inconsequential to being dominant. These are cliff events on the plots. The cell dies as the difference between the two half-cell potentials diminishes. Equilibrium, another term for a dead battery, is rapidly approached.

Author Information

Corresponding Author

*E-mail: garon.smith@umontana.edu

ORCID

Garon C. Smith: 0000-0003-0145-8286

Acknowledgments

The authors are grateful to the Department of Chemistry and Biochemistry at The University of Montana for financial support of a graduate teaching assistantship during the course of these studies.

References

1. Smith, G. C., Hossain, M. M.; MacCarthy, P. Why Batteries Deliver a Fairly Constant Voltage Until Dead. *J. Chem. Educ.*, **2012**, 89(11), 1416-1420. <http://pubs.acs.org/doi/abs/10.1021/ed200211s>.
2. Nernst, W. Z. Die elektromotorische Wirksamkeit der Ionen. *Phys. Chem.* **1889**, 4, 129-181. <https://doi.org/10.1515/zpch-1889-0412>

3. Peters, R. Z. Ueber Oxydations- und Reduktionsketten und den Einfluss komplexer Ionen auf ihre elektromotorische Kraft. *Phys. Chem.*, **1898**, *26*, 193-236.
<https://doi.org/10.1515/zpch-1898-2618>
4. Harris, D. *Quantitative Chemical Analysis*. 8th Edition; Freeman: New York, 2010, AP20-AP27. ISBN: 14292181505.
5. Smith, M. J.; Gray, F. Batteries, from Cradle to Grave. *J. Chem. Educ.*, **2010**, *87*(2), 162–167.
<https://doi.org/10.1021/ed800053u>
6. McMurry, J.; Fay, R. *Chemistry*, 3rd ed.; Prentice Hall: Upper Saddle River, NJ, 2001; p 784. ISBN 13: 978-0130872050.
7. Chambers, J. Q. Electrochemistry in the general chemistry curriculum. *J. Chem. Educ.*, **1983**, *60*(4), 259–262.
<https://doi.org/10.1021/ed060p259>
8. Ciparlick, J. D. Half cell reactions: Do students ever see them? *J. Chem. Educ.*, **1991**, *68*(3), 247.
<https://doi.org/10.1021/ed068p247.1>
9. Probst, D. A.; Henderson, G. Zinc Electrodes and the Thermodynamics of a Galvanic Cell. *J. Chem. Educ.*, **1996**, *73*(10), 962–964.
<https://doi.org/10.1021/ed073p962>
10. Mills, K. V.; Herrick, R. S.; Guilmette, L. W.; Nestor, L. P.; Shafer, H.; Ditzler, M. A. Introducing Undergraduate Students to Electrochemistry: A Two-Week Discovery Chemistry Experiment. *J. Chem. Educ.*, **2008**, *85*(8), 1116–1119.
<https://doi.org/10.1021/ed085p1116>
11. Peckham, G. D.; McNaught, I. J. The Variation of Electrochemical Cell Potentials with Temperature. *J. Chem. Educ.*, **2011**, *88*(6), 782–783.
<https://doi.org/10.1021/ed100966r>
12. Treptow, R. S. The Lead-Acid Battery: Its Voltage in Theory and in Practice. *J. Chem. Educ.*, **2002**, *79*(3), 334–338.
<https://doi.org/10.1021/ed079p334>
13. Lamb, R. E.; Natusch, D. F. S.; O'Reilly, J. E.; Watkins, N. Laboratory experiments with ion selective electrodes. *J. Chem. Educ.*, **1973**, *50*(6), 432–434.
<https://doi.org/10.1021/ed050p432>
14. Light, T. S.; Cappuccino, C. C. Determination of fluoride in toothpaste using an ion-selective electrode. *J. Chem. Educ.*, **1975**, *52*(4), 247– 250.

- <https://doi.org/10.1021/ed052p247>
15. Meyerhoff, M. E.; Kovach, P. M. An ion-selective electrode/flow-injection analysis experiment: determination of potassium in serum. *J. Chem. Educ.*, **1983**, *60*(9), 766–768.
<https://doi.org/10.1021/ed060p766>
 16. Li, G.; Polk, B. J.; Meazell, L. A.; Hatchett, D. W. ISE Analysis of Hydrogen Sulfide in Cigarette Smoke. *J. Chem. Educ.*, **2000**, *77*(8), 1049–1052.
<https://doi.org/10.1021/ed077p1049>
 17. Harris, D. *Quantitative Chemical Analysis*. 8th Edition; Freeman: New York, 2010, p. 172. ISBN: 14292181505.
 18. MacCarthy, P. Classification of experimental methods in solution chemistry. *J. Chem. Educ.*, **1986**, *63*(4), 339–343.
<https://doi.org/10.1021/ed063p339>